IEEE Access
Multidisciplinary : Rapid Review : Open Access Journal

Received July 20, 2020, accepted July 29, 2020, date of publication August 3, 2020, date of current version August 14, 2020.

Digital Object Identifier 10.1109/ACCESS.2020.3013657

Review of Substation Grounding System Behavior Under High Frequency and Transient Faults in Uniform Soil

NAVINESSHANI PERMAL[1], MISZAINA OSMAN[1], (Senior Member, IEEE), MOHD ZAINAL ABIDIN AB. KADIR[1,2], (Senior Member, IEEE), AND AZRUL MOHD ARIFFIN[1], (Member, IEEE)

[1]Institute of Power Engineering, Universiti Tenaga Nasional, Kajang 43000, Malaysia
[2]Center for Electromagnetic and Lightning Protection Research (CELP), Advance Lightning, Power and Energy Research (ALPER), Universiti Putra Malaysia, Seri Kembangan 43400, Malaysia

Corresponding author: Navinesshani Permal (nesshani@yahoo.com)

This work was supported by the UNITEN BOLD Postgraduate Scholarship Programme.

ABSTRACT Substations are important parts of electric power systems, and they require well-designed grounding systems. A proper grounding system guarantees the safety of the personnel working in an environment surrounded by grounded equipment from possible electric shock, protects the equipment against unnecessary breakdowns, and conserves the stability of the entire electrical system throughout its operation. Grounding systems developed under power frequency conditions generally react differently under high frequency and transient conditions, such as switching transients and lightning strikes. This work reviews the modeling methods for substation grounding systems and their performance when grounding design parameters change under high frequency and transient fault conditions.

INDEX TERMS Substation grounding, grounding, transient faults, lightning, uniform soil.

I. INTRODUCTION

Electrical grounding systems are important in creating a safe environment for human operators and equipment under fault or transient conditions. Electrical installation must be grounded for the following reasons [1]–[8]:

- It provides a low impedance path between the electrical equipment and the ground;
- It provides a reference potential for electrical equipment;
- It prevents extreme overvoltage and potential gradients that might harm the human personnel working around it and damage the power equipment.

Generally, any fault current in a power substation flows through the ground via a ground electrode system, which has an impedance to the current flow. The impedance causes the voltage of the ground electrode system to increase. The potential difference created by the excessive voltage increase might cause equipment damage and endanger the lives of humans and animals in the proximity of the grounded system [9]. Grounding designs and procedures under power frequencies are comprehensively described in many standards [10]–[13].

The associate editor coordinating the review of this manuscript and approving it for publication was Yanbo Chen.

The behaviors of grounding systems under high frequency and transient conditions are different from those under conventional power frequency conditions. For example, a grounding system exhibits different behaviors when lightning current passes through the grounding system. This condition is caused by the inductive and capacitive effects on the grounding system. A huge lightning current with a fast rise time flows to the grounding grid, which induces large transient voltages in the system. The resulting voltages can create a huge potential rise and electromagnetic coupling, which lead to system breakdowns and errors, especially in important and sensitive electronic equipment in power substations [3], [14]–[16].

Therefore, the research on grounding system behavior under high frequency and transient conditions is essential to enhance the performance and design of grounding system. Numerous studies have explored actual grounding systems and laboratory-scale models [8], [17]–[32]. Although experiments can clarify actual grounding operations, they require a large space, which reflects high costs. Thus, numerical modeling methods using computer simulations have been utilized as a solution to expensive lab space restrictions. Numerical models can be categorized into four types, namely electric

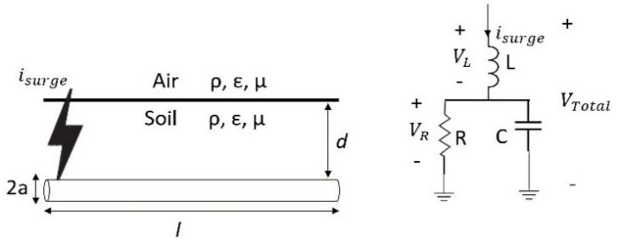

FIGURE 1. Equivalent lumped circuit model for a vertical grounding electrode under lightning current [38].

circuit models, transmission line (TL) models, electromagnetic models and hybrid models.

II. MODELING METHODS OF GROUNDING SYSTEMS

Theoretically, most numerical models for grounding transient analysis can be categorized as follows [33]–[35]:

1) Electric circuit models
2) Transmission line models
3) Electromagnetic models
4) Hybrid models

Electric circuit models [28], [36]–[39] are similar to basic circuit models which are based on nodal analysis and Kirchoff's law for lumped circuits identified for each small segment of grounding conductors. Initially, these models treated grounding grid segment parameters as frequency independent. The first circuit model was proposed in [40].

Nodal analysis was applied to that model for frequency-independent circuit elements of small segments. The equations were solved on the basis of a Laplacian equation. Further improvements through research include the frequency dependence of internal resistance, capacitance a, self- and mutual inductance, and conductance [41].

The proposed model was improved later using Maxwell's equations to consider the impact of frequency on the parameters of grounding systems [42]. A modest model for grounding systems that considers mutual effects was proposed in [43]. Then, a few equivalent circuit models in [44] were compared with other previous models to take the soil ionization effect into account. A lumped circuit model [45] was recommended to simulate grounding electrodes under transient conditions. The Resistor (R), Inductor (L), Capacitor (C) model (RLC) can easily be simulated in transient programs, such as the Electromagnetic Transients Program (EMTP). Fig. 1 shows an identical lumped circuit model of a typical grounding electrode. It does not contemplate wave propagation delay and comprises only one section of RLC components.

In Fig. 1, the current affects the grounding electrode and flows into the ground thereby adding to the resistivity; and has a dielectric constant, ε. Thus, conductive current in the ground is developed when the electrode voltage changes with time. The capacitive current follows the conductive current path; therefore, the ground electrode gains capacitance, that reciprocates the resistance shown in (1) and (3) [46]. The inductance of such a rod is calculated using (2). The conventional expressions of ground resistance (R), inductance (L), and capacitance (C) for a vertical rod are respectively given by the following equations [3], [47]–[49] with the assumptions of $l \gg a$ and $l \gg d$:

$$R = \frac{\rho}{2\pi l}[\ln\left(\frac{4l}{a}\right) - 1] \tag{1}$$

where ρ is the soil resistivity in [Ω.m], l is the length of the electrode in [m], a is the radius of the electrode in [m], and d is the burial depth in [m]:

$$L = \frac{\mu l}{2\pi}[\ln\left(\frac{2l}{a}\right) - 1] \tag{2}$$

where μ is the soil permeability ($4\pi \times 10^{-7}$ H/m), l is the length of the electrode in [m], and a is the radius of the electrode in [m]:

$$C = \frac{\rho\varepsilon}{R} \tag{3}$$

where ρ is the soil resistivity in [Ω.m], ε is the permittivity of soil in [F/m], and R is the ground resistance calculated using (1).

Electric circuit models can be easily designed in circuit–based programs, their mutual impedances can be included in calculations, and their nonlinear elements can be considered [38]. However, circuit models are unable to forecast surge propagation delays and the accuracy of their transient voltage responses is not as high as that of electromagnetic field models [37], [38], [49], [50].

TL models (TL) [48], [22], [51]–[56] which can be considered as an extension of circuit models are highly applicable, simple and computationally efficient. Some of TL models are suitable for the resolutions in time domain, whereas others are effective in the frequency domain. The first TL models were proposed in [57]. A horizontal wire was serving as a grounding system was modeled on the basis of the loss TL concept with the same transient characteristics as an overhead transmission line as defined by the telegrapher's equations [7].

The typical TL model has been protracted from basic grounding wires to grounding grids, and enhanced from uniform to nonuniform per-unit parameters [48], [58]. This model can be computed in the time or frequency domain and it can comprise mutual couplings between grounding wires, as well as soil ionization.

A uniformly distributed model is used to consider the nonuniform distribution of the current along electrodes (Fig. 2). This model is divided into lumped models separated into N sections. VLi is the inductive voltage at each section.

The number of sections should be considered to determine the RLC values of the distributed model for each segment. Typically, each meter of ground electrode is equal to one section. Therefore, the per-unit length distribution of parameters for each section is approximately determined as follows:

$$R' = Rl \tag{4}$$

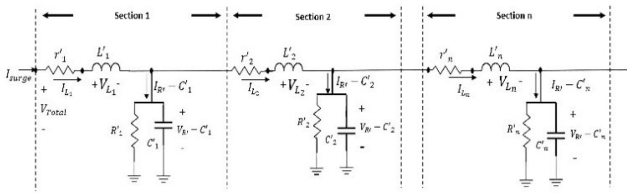

FIGURE 2. Distributed model of grounding system [59].

$$C' = \frac{C}{l} \tag{5}$$

$$L' = \frac{L}{l} \tag{6}$$

$$r' = \frac{\rho_c}{l\pi a^2} \tag{7}$$

where R, C, and L are obtained by (1) to (3) in the circuit model approach, r' is the electrical resistance of the per- unit length electrode (in Ω), ρ_c is the electrical resistivity of the electrode (in Ω.m), and a is the electrode radius (in metre).

TL models are regarded as the least accurate among all four models. The main disadvantage of TL models is that they cannot produce an accurate transient voltage response in grounding systems.

Nevertheless, TL models are highly applicable, simple, and computationally efficient. They also satisfy engineering requirements as they can be modeled in transient programs such as EMTP. In addition, they are quick to perform computations, and they are easy to formulate [54], [60].

Electromagnetic models [49], [61]–[64] are said to be the most accurate because they use Maxwell's equations to solve problems with the least assumptions [65], [66]. The equations can be solved using the Method of Moment (MoM), Finite-Difference Time-Domain (FDTD), and Finite Elements Method (FEM).

However, numerical calculations of these approaches are extremely heavy and time-consuming [50]. In the MoM, Maxwell's equations are used to derive the integral equations as the boundary conditions of a system [67]. These integral equations need to be solved using linear numerical methods. In this case, a grounding system should be divided into N, small and equal segments such that the approximation of a linear system can be achieved. This requirement is due to the magnitude of the current which is considered constant in conductors. The first investigation about grounding systems based on the electromagnetic model using antenna theory was carried out by Miller [67].

The MoM technique operates in the frequency domain, which computes based on the residual weight that solves an integral equation. The simulation of the technique needs to be carried out in the frequency domain via Fourier transform with discretized time-domain data according to sampling time. The solution solved using the MoM represents the problem by using Sommerfeld integral form. Most importantly, current distributions for every segment of the grounding conductor were solved using the MoM, followed by the calculation of leakage current and electric fields surrounding the conductor. Potentials at different reference points can be calculated by integrating the electric field from the surface of the conductor to the remote earth. Although this method can generate accurate data, it takes a significant amount of computer memory for computation and, concurrently, the nonlinear behavior of the soil in the frequency domain will be complicated to compute.

The MoM starts with (8) to compute the distributed electric field:

$$E_s = \frac{1}{4\pi j\omega\varepsilon^*}(\nabla\nabla - \gamma_1^2 \int_l t'.I_l\left(r'\right).G_n\left(r.r'\right)dl \tag{8}$$

where E_s is the total dispersed electric field along the surface of the conductor. $t'.I_l\left(r'\right)$is the flow of current along the conductor. $G_n\left(r.r'\right)$ is the complete Green function. ε^* is the complex permittivity and γ is the wave propagation constant.

FDTD is based on the discretisation of Maxwell's equation directly in both time and space to rectangular cells. Each electric field component was situated at a half-cell width from the origin in the direction of its position, while each magnetic field component was in a counterbalance from the center of three faces of the cell. Hence, a solution was achieved in the time domain, and solving linear equations were unnecessary because FDTD seemed to need less computational time than other numerical methods. The disadvantages of this method were cubical meshing, where there were problems when the requirements of curve geometry and small time steps arise [68].

The FEM resolves differential or integral equations by discretizing the volume-space and applying the equations to the surfaces characterized by volume-space points before resolving the subsequent matrices. The advantage of the method is that an electromagnetic field can be calculated at any point within the boundary of the model. Therefore, the simulation has additional ability to calculate the grounding impedance at the injection point. The major challenge is the meshing procedure, simply because the geometry contains very small and long grid conductors coupled with large boundaries. Besides, the reflections from the boundary need to be avoided to simulate the open boundary problems [22].

Electromagnetic models are only aimed at transforming the related electric field based on Maxwell's equations into a linear algebraic equation system with the least presumptions. Miller also proposed the reflection coefficient model and the transmitted coefficient model to boost computation speeds [69], [70].

Hybrid models [62], [71]–[74] are combinations of electric circuit models and electromagnetic models based on Partial Element Equivalent Circuit (PEEC) [35], [37] and Hybrid Electromagnetic Method (HEM) [75]. PEEC can solve in both time and frequency domain. The integration of the electric field along a defined path calculated the potential value. It can include electrical components such as transformers, resistive, inductive, and capacitive (RLC) elements, transmission lines, and cables which are based on circuit theory.

TABLE 1. Summary of grounding modeling methods.

Model	Fundamental of computation	Concept and solutions	Benefits	Drawbacks
Electric circuit	Nodal analysis, Kirchoff's law	Simple	can be easily designed in circuit-based programs, the mutual impedances can be included in calculations, and the nonlinear elements can be considered	cannot predict the surge propagation delay, the accuracy of the transient voltage response is not as high as the electromagnetic field model
Transmission line	Telegrapher's equations	Simple	more applicable, simple, and fast in computation and it satisfies the engineering aspects as it can be modeled in transient programs such as EMTP	least accurate, it cannot produce the accurate transient voltage response of the grounding systems
Electromagnetic	EM computation, Maxwell's equations, MoM, FEM, FDTD solution	Complex	most accurate and with least assumptions	numerical calculations are extremely heavy and time-consuming
Hybrid	Maxwell's equations, Transform equations, PEEC and HEM solution	Complex	able to foresee all the important parameters of transient behavior.	it cannot be used in circuit-based standard programs to show the influence of the grounding systems on power system equipment

HEM is named after adopting a dual approach (Electromagnetic and Circuit). First, couplings are assessed from a numerical execution of basic electromagnetic (EM) equations. Then, the continuity of current is applied to provide an answer for circuital quantities. The HEM method equalizes well between precision and competence of the computational code that executes the model algorithm. From an engineering view, a grounding systems model developed for the transient analysis should be modest for fast and accurate applications.

Hybrid models require heavy numerical computations to solve equations, especially when the analysis involves large systems. These models consider the impact of frequency variations on series internal impedances, inductive components, and capacitive-inductive components. Hence, these models are more precise than conventional electric circuit models particularly when the frequency at the injection point is high. The basic electromagnetic equation for an energized grounding conductor [67] is given as:

$$Z_k I_k + j\omega \sum\nolimits_{i=1}^{n} A_{ik} + \sum\nolimits_{i=1}^{n} \frac{\partial \varphi_{ik}}{\partial v} = 0 \tag{9}$$

The equation generates a set of linear equations, which can be used to determine the current distribution in n conductor segments. Z_k is the internal impedance of the *kth* segment. I_k is the current in the *kth* segment. A_{ik} *is* the vector potential. Φ_{ik} *is* the scalar potential, v *is* any point on the surface of the *kth* segment, and ω *is the* angular frequency. The internal impedance Z_k is obtained as:

$$Z_k = \frac{j\omega\mu}{2\pi r\sqrt{j\omega\mu\sigma}} \cdot \frac{I_0(r\sqrt{j\omega\mu\sigma})}{I_1(r\sqrt{j\omega\mu\sigma})} \tag{10}$$

where r is the radius, μ is the permeability, and σ is the conductivity of the copper conductor segment k. I_0 and I_1 are the zero and first-order Bessel's functions of the first kind.

For each segment, (11) can be written in the form of an equivalent circuit using a hybrid model [76]:

$$Z_k I_k + j\omega \sum\nolimits_{i=1}^{n} A_{ik} + \sum\nolimits_{i=1}^{n} \varphi_k - \varphi_i = 0 \tag{11}$$

where φk and φi are the average scalar potentials on the surface of segments k and i, respectively.

This model can forecast all important features of lightning-induced transient behavior. For example, in an analysis, evaluating soil ionization is more important than treating boundary conditions. The drawback is that the model cannot be used in circuit-based standard programs to show the influence of grounding systems on power system equipment. Table 1 presents a summary of the concepts, benefits, and drawbacks of the different grounding modeling methods.

With the advancement of modeling understanding and capabilities provided by software developers, the accurate representation of the modeling methods listed in Table 1 can be implemented in real equipment or practical scenarios. In this implementation, the design details of systems are considered along with several assumptions and limitations in accordance with standard recommendations that are in good agreement with measured works. Simulation packages such as power system computer-aided design/EMTP, and Current Distribution, Electromagnetic Interference, Grounding, and Soil Structure Analysis (CDEGS) provide a platform for users to model and represent the behavior of the same object based on its theoretical model. Furthermore, these modeling approaches extend existing works to be carried outside laboratory. For instance, with the option to vary and change the design parameters (configuration, dimension and material) and level of disturbances (magnitude and waveform), one can predict the behavior and performance of systems installed without worrying about damage and installation costs. Hence, the most appropriate solutions, can be achieved through simulation and practical installation.

III. INFLUENCE OF DESIGN PARAMETERS ON GROUNDING SYSTEM BEHAVIOR

The behaviors of grounding systems under high frequency and transient fault conditions are unlike from those under power frequency fault conditions. The power frequency fault currents can vary from a few kA up to 20–30 kA [77].

Moreover, ground impedances of high voltage substations range from 0.05 Ω to 1 Ω. Although high fault current magnitudes are commonly related to low ground impedances, ground potential can increases as high as several tens of kV [77]. Thus, working personnel in the proximity of power systems face the risk of possible electrocution during earth faults, and equipment damage is likely unless precautionary actions are taken to restrict ground potential rise and control potential differences in high-risk zones.

High magnitude currents of several tens of kA under transient fault conditions such as direct lightning strikes, flow to the earth through grounding systems, leading to large potential gradients: in such a case, grounding systems exhibit a potential rise relative to the reference earth and power systems should thus be secured against overvoltage [78]. The flow of transient currents into earth may also cause an electric shock risk but their acceptable limits are not as well defined as those of power frequency fault currents.

The main parameters accountable for grounding system behavior under transient conditions can be categorized into: the association between the power system and the electrodes, which should be as short as possible [79]; the design of the grounding system, including the electrode type, length, and sizes; and the characteristics of the earth (soil resistivity) where the grounding grids are established. The investigation results of these parameters provide useful guidance for installing grounding electrodes, measuring and testing grounding systems' performances and for achieving an effective design of the substation grounding systems.

A basic grounding performance analysis includes the design parameters of grounding grids and soil characteristics. Grounding impedance relies on the size and shape of the grid, spacing between electrodes, current injection point, wave shape and magnitude of the current and characteristics of soil. Considering uniform soil, we discuss the factors of grounding design parameters that influence grounding impedance and ground potential rise in following sections.

A. EFFECT OF GRID SIZE

This section confers the impact of grid size on grounding grid impedance. Grid size is the total size of conductors covered by the grounding grid [23], [80], [81]. Fig. 3 shows the impedance magnitudes at various frequencies under high and low soil resistivity. The grid impedance is almost constant (resistive behavior) until a certain frequency which is referred to as the "upturn" frequency.

Beyond the upturn frequency, the magnitude of grid impedance starts to increase fast as the frequency increases. The particular frequency at which the grid impedance begins

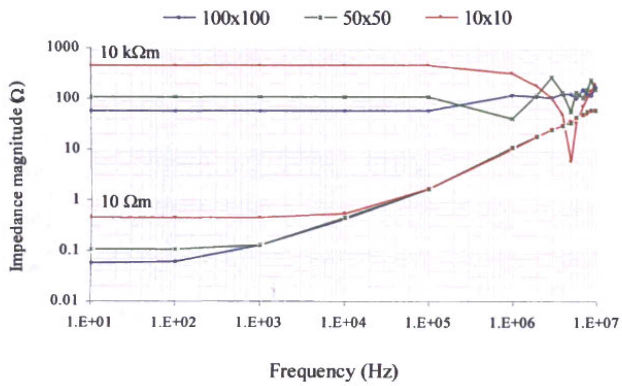

FIGURE 3. Impedance magnitude at various frequencies for different grid sizes [82].

TABLE 2. Summary of effects of grid size on grounding grid impedance.

Frequency	Soil resistivity	Effect of grid size on grounding grid impedance
Low	Low	Less reduction
	High	Significant reduction, higher magnitude compared to low resistivity
High	Low	Slight reduction
	High	Almost constant, higher magnitude compared to low resistivity

to increase is called the upturn frequency. It also confide on the grounding grid dimensions and the medium of soil resistivity [82]. For low soil resistivity (10 Ω.m), the grid impedance begins to decrease (inductive effect) at 100 Hz for a 10 m x 10 m grid, and at 10 kHz for 100 m x 100 m grid. By contrast, high resistivity soil (10 kΩ.m), has no upturn frequency, and the grid impedance is almost constant for a high frequency condition (100 kHz). However, the impedance of increasing grid sizes does not converge at a high frequency.

The graphs in Fig. 4(a) and Fig. 4(b) show that the grid impedance decreases greatly as grid size increases at a low frequency. Moreover, the grid impedance decreases slightly as the grid size increases before reaching a constant value at a low frequency (100 kHz) under low soil resistivity (100 Ω.m).

Beyond 10 m x 10 m at 1 MHz and 100 Ω.m soil resistivity, the grid impedance is constant as it has reached its effective area. A similar behavioral pattern can be observed at high soil resistivity. A summary of the effects of grid size on grid impedance is presented in Table 2.

B. EFFECT OF OVERALL MESH DENSITY

In a grounding grid, a mesh is referred to as the separation between conductors. This mesh is designed to minimize the possible increase in step and touch voltages. Grid mesh density can vary uniformly across the grid or it may be enhanced locally within areas of the grid. Mesh density exerts a significant effect at an intermediate frequency, under which it is determined by soil resistivity [81], [84]–[87]. Fig. 5

TABLE 3. Impedance magnitude at different frequencies for overall mesh density.

Frequency (Hz)	Soil resistivity (10Ω.m)				Soil resistivity (100Ω.m)				Soil resistivity (1000Ω.m)			
	No. of mesh				No. of mesh				No. of mesh			
	4	16	100	400	4	16	100	400	4	16	100	400
10	0.08Ω	0.07Ω	0.06Ω	0.05Ω	0.8Ω	0.7Ω	0.6Ω	0.5Ω	8Ω	7Ω	6Ω	5Ω
100	0.08Ω	0.07Ω	0.06Ω	0.05Ω	0.8Ω	0.7Ω	0.6Ω	0.5Ω	8Ω	7Ω	6Ω	5Ω
1k	0.1Ω	0.1Ω	0.1Ω	0.1Ω	0.8Ω	0.7Ω	0.6Ω	0.5Ω	8Ω	7Ω	6Ω	5Ω
10k	0.5Ω	0.5Ω	0.5Ω	0.5Ω	1Ω	1Ω	1Ω	1Ω	8Ω	7Ω	6Ω	5Ω
100k	2Ω	2Ω	2Ω	2Ω	8Ω	8Ω	8Ω	8Ω	10Ω	10Ω	10Ω	10Ω
1M	10Ω	10Ω	10Ω	10Ω	11Ω	11Ω	11Ω	11Ω	60Ω	60Ω	60Ω	60Ω
10M	80Ω	80Ω	80Ω	80Ω	90Ω	90Ω	90Ω	90Ω	100Ω	100Ω	100Ω	100Ω

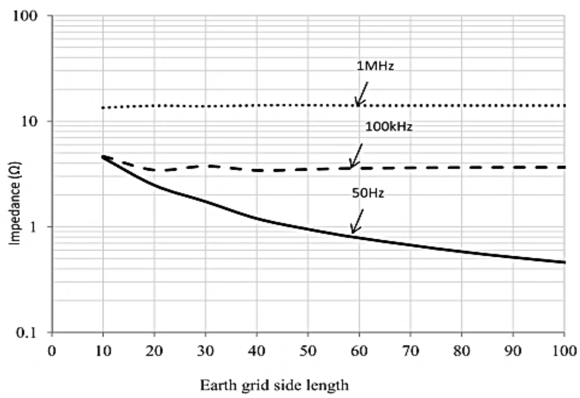

(a). Effect of grid size on grid impedance at 100 •.m soil resistivity [83].

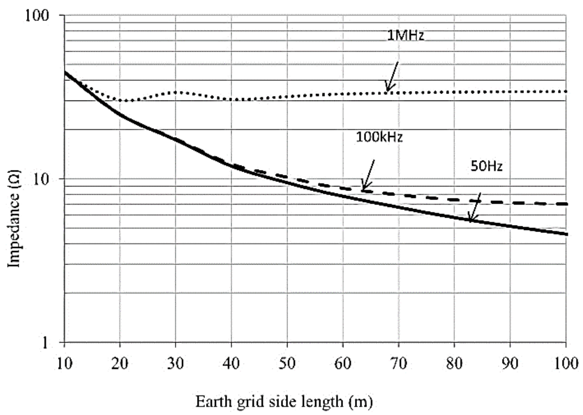

(b). Effect of grid size on grid impedance at 1k •.m soil resistivity [83].

FIGURE 4. (a) Effect of grid size on grid impedance at 100 Ω.m soil resistivity [83]. 4(b) Effect of grid size on grid impedance at 1k Ω.m soil resistivity [83].

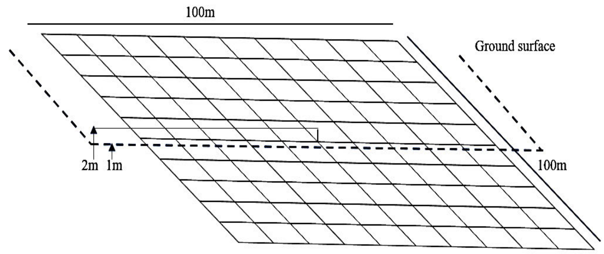

FIGURE 5. Overall mesh density of 100m x 100m grounding grid with 100 meshes [88].

TABLE 4. Summary of effects of overall mesh density on grounding grid impedance.

Frequency	Soil resistivity	Effect of mesh density on grounding grid impedance
Low	Low	Less reduction
	High	Less reduction, higher magnitude compared to low resistivity
High	Low	Almost constant
	High	Significant reduction, higher magnitude compared to low resistivity

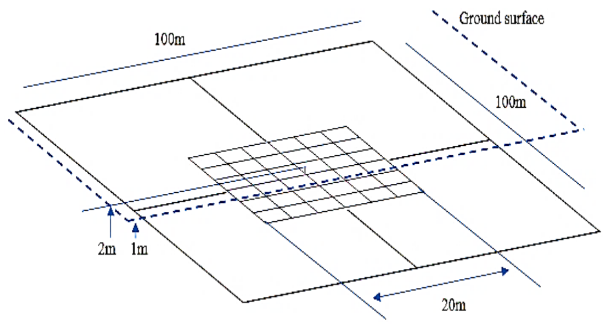

FIGURE 6. Local mesh density of 100 m x 100 m grounding grid with 4+36 meshes [90].

shows the overall mesh density of a 100 m x 100 m grid with 100 meshes.

Table 3 represents the impedance magnitudes at different frequencies for a 100 m x 100 m grounding grid under various overall mesh densities value [88].It shows that the effect of the overall increasing mesh density becomes noticeable between between 100 Hz and 10 kHz; at 1 kHz, the mesh density reaches its maximum value for low soil resistivity (10 Ω.m). For high soil resistivity (1000 Ω.m), the decrease of the grid impedance reaches the peak value at 100 kHz. This behavior could be associated with different effective areas of the grounding system as soil resistivity varies. A summary of the effects of overall mesh density on grid impedance is presented in Table 4.

C. EFFECT OF LOCAL MESH DENSITY

Fig. 6 shows the local mesh density of a 100 m x 100 m grid with extra 46 meshes. Table 5 represents the impedance

TABLE 5. Impedance magnitude at various frequencies for different local mesh density.

Frequency (Hz)	10Ω.m			1kΩ.m		
	4 + 36 mesh	4 + 4 mesh	4 mesh	4 + 36 mesh	4 + 4 mesh	4 mesh
10	0.08Ω	0.08Ω	0.08Ω	8Ω	8Ω	8Ω
100	0.08Ω	0.08Ω	0.08Ω	8Ω	8Ω	8Ω
1k	0.1Ω	0.1Ω	0.1Ω	8Ω	8Ω	8Ω
10k	0.4Ω	0.5Ω	0.6Ω	8Ω	8Ω	8Ω
100k	2Ω	2Ω	2Ω	10Ω	10Ω	10Ω
1M	9Ω	9Ω	9Ω	50Ω	40Ω	30Ω
10M	70Ω	70Ω	70Ω	200Ω	200Ω	200Ω

TABLE 6. Summary of effects of local mesh density on grounding grid impedance.

Frequency	Soil resistivity	Effect of mesh density on grounding grid impedance
Low	Low	Almost constant
	High	Almost constant, higher magnitude compared to low resistivity
High	Low	Less reduction
	High	Significant reduction, higher magnitude compared to low resistivity

magnitudes at various frequencies for a 100 m x 100 m grounding grid under different local mesh density [88]. The grid is enhanced with local mesh density under low soil resistivity (10 Ω.m) and high soil resistivity (1 kΩ.m). The overall mesh density of the grounding grid behaves similarly to the improved local mesh density. The magnitude of the grid impedance is less influenced by the local mesh density than by overall mesh density at a low frequency under low and high soil resistivity.

The decrement in grid impedance is barely noticeable. Meanwhile, the reduction of grid impedance with the increase in local mesh density depends on soil resistivity at a high frequency. Under low soil resistivity (10 Ω.m), the impedance magnitude decreases as the local mesh density increases for frequencies between 1 kHz and 100 kHz. A significant reduction can be observed at high soil resistivity. Table 6 presents a summary of the effects of local mesh density on grid impedance.

D. EFFECT OF NUMBER OF ELECTRODES

Attaching electrodes at the grid boundary is one of the suggestions given by IEEE 80 [10] and EA 41-24 [79] standards to enhance the power frequency performance. However, under transient conditions, the standards suggest that the electrodes should be attached directly below the current injection location, where the transient currents flow into the [89]–[93].

Fig. 7 shows a 12 m x 12 m 16-mesh grid buried at a depth of 1 m and a current injected into the center of the grid through a 3.3 m downlead conductor located above ground. Initially, five electrodes are added to this model; the first electrode is placed at the center just below the injection point, and

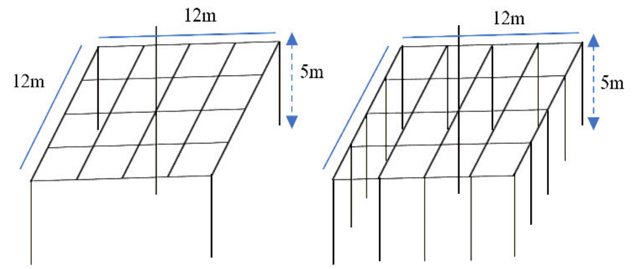

FIGURE 7. Ground grid configurations with different numbers of electrodes [94].

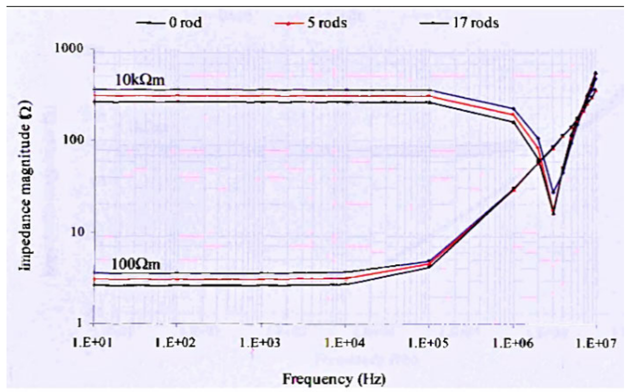

FIGURE 8. Impedance magnitude at various frequencies for a different numbers of electrodes [94].

the rest of the electrodes are positioned at the corners of the grid. Other electrodes are added to the grid and are uniformly dispersed around the perimeter of the grid. The total number of electrodes is increased to seventeen, and each electrode measures 5 m in length.

Fig. 8 shows the impedance magnitude of electrode arrangements for different soil resistivities and frequencies. The grid impedance decreases for all soil resistivities when the electrodes are added. In high soil resistivity, the addition of rods reduces the grid impedance at a high frequency of up to 4 MHz. Beyond this frequency, the impedance magnitude for all grids converges similarly to that under low soil resistivity. This study shows that adding five electrodes results in an estimated reduction of 14% in grid impedance for all soil resistivities and that increasing the number of electrodes to 17 causes a 26% reduction in the magnitude of grid impedance when no additional electrodes are added. Table 7 presents a summary of the effects of number of electrodes on grounding grid impedance.

E. EFFECT OF LENGTH OF ELECTRODE

Extensive research evaluated the impact of ground electrodes length on the performance of grounding systems [18], [24], [83], [89], [95]. This section presents the effects of different lengths (vertical ground electrodes; 5, 10, 15 and 20 m; horizontal ground electrodes; 10, 20, 40 and 50 m) on grid impedance. The electrodes are made of copper and are buried

TABLE 7. Summary of effects of number of electrodes on grounding grid impedance.

Frequency	Soil resistivity	Effect of the number of electrodes on grounding grid impedance
Low	Low	Less reduction
	High	Less reduction, higher magnitude compared to low resistivity
High	Low	Almost constant
	High	Significant reduction, higher magnitude compared to low resistivity

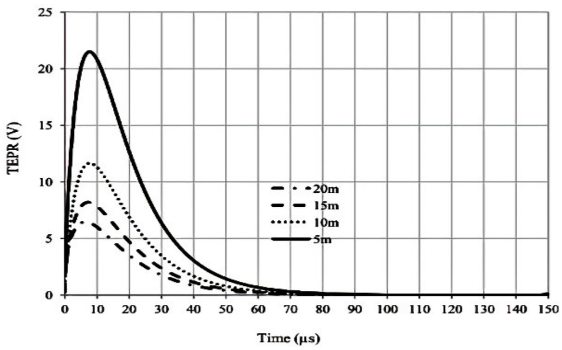

(a). Effect of electrode length on the TEPR of vertical electrodes [83].

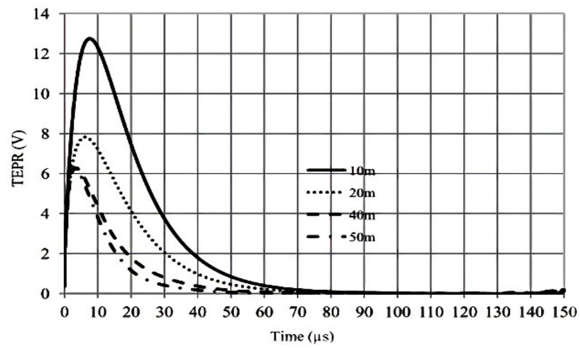

(b). Effect of electrode length on the TEPR of horizontal electrodes [83].

FIGURE 9. (a) Effect of electrode length on the TEPR of vertical electrodes [83]. (b) Effect of electrode length on the TEPR of horizontal electrodes [83].

at a depth of 1 m into the soil with an impulse current of 8/20 μ s injected at one end. The results, with transient earth potential rise (TEPR) as a function of time, are shown in Fig. 9(a) and Fig. 9(b) [83].

Fig. 11(a) shows that the TEPR decreases as the vertical electrode length increases. Fig. 9(b) shows that the TEPR decreases as the horizontal electrode length increases. The increase of the vertical electrode length from 5 m to 20 m causes a significant reduction of approximately 70% in the TEPR as shown in Fig. 9(a). A similar pattern can be observed for the horizontal electrode with lengths ranging from 10 m to 50 m (Fig. 9(b)). The effective length of the horizontal electrode is reached at 40 m as no further reduction in TEPR is gained beyond this length.

Fig. 10 compares the contrast between 5 and 10 m vertical electrodes over a series of frequencies for two different soil resistivities (100 Ω.m and 10 kΩ.m). For a 10 m

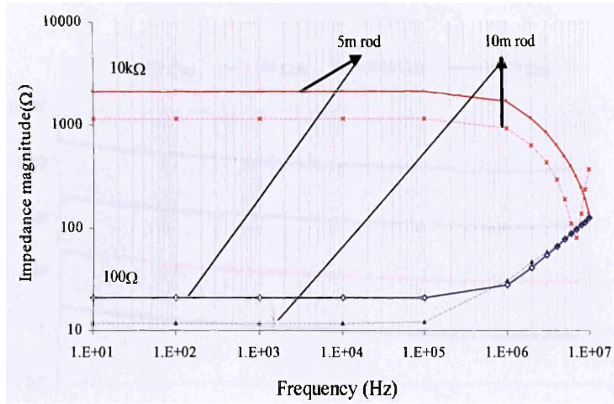

FIGURE 10. Impedance magnitude at various frequencies for different lengths of vertical electrodes [94].

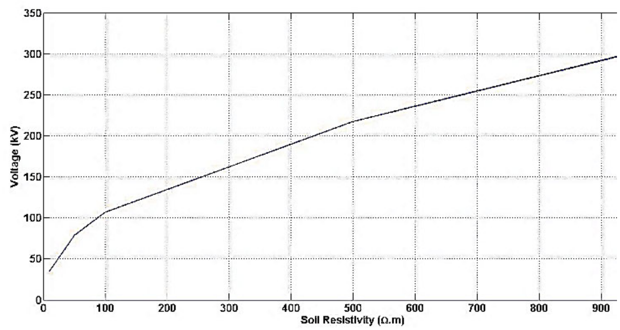

FIGURE 11. Peak voltage for different soil resistivities with an injected current of 10 kA 1.2/50. μs at the corner of a 20 m x 20 m grounding grid [100].

TABLE 8. Summary of effects of electrode length on grounding grid impedance.

Frequency	Soil resistivity	Effect of length of electrode on grounding grid impedance
Low	Low	Less reduction
	High	Less reduction, higher magnitude compared to low soil resistivity
High	Low	Almost constant
	High	Significant reduction, long electrodes have lower magnitude compared to short electrodes

vertical electrode, the impedance is smaller than that for a 5 m vertical electrode. For a low soil resistivity medium, the grid impedance of the 5 m vertical electrode is double of the grid impedance of a 10 m vertical electrode. For a high soil resistivity medium, the impedance magnitude of the 10 m electrode is about 55% of that of the 5 m electrode for frequencies of up to 5 MHz. The ground impedance of 10 m electrode beyond 5 MHz increases as the frequency increases [85]. Table 8 shows the effects of electrode length on grid impedance.

F. EFFECT OF SOIL RESISTIVITY

Soil resistivity is one of the most important parameters determining the type of soil to establish a grounding system. Generally, soil resistivity is subjected to the chemical content, temperature, geography and water content of the soil [19],

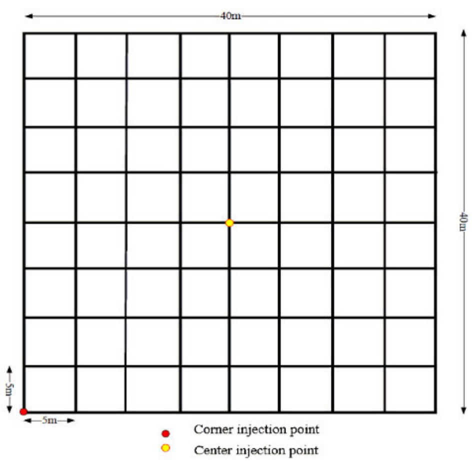

FIGURE 12. Location of injection point [23].

[35], [83], [84], [96]–[99]. In this section, the values ranging from 10 Ω.m to 1000 Ω.m are used to further study the effects of soil resistivity. A lightning current of 10 kA with a 1.2/50 μs voltage waveform is injected through the down conductor to the corner of the grid. The depth of grid buried under soil is 0.5 m. The grid size is 20 m x 20 m and the mesh size is 5 m x 5 m. Fig. 11 shows the peak ground potential rise for various soil resistivities. The potential peak magnitude in 10 Ω.m soil resistivity is about 35k V, which gradually increases with high soil resistivity. For example, the ground potential rise is about 310 kV when the soil resistivity is 1000 Ω.m.Therefore, low soil resistivity is important in good grounding design.

IV. INFLUENCE OF LIGHTNING CURRENT AND WAVEFORM PROPERTIES ON GROUNDING SYSTEM BEHAVIOR

In addition to grid geometry, design and soil parameters, lightning properties such as the current injection location and the waveform of current impulse play a vital part in determining the grounding grid performance.

A. EFFECT OF THE CURRENT INJECTION POINT

The grounding system behavior under transient conditions can be enhanced through the positions of the current injection point because they can create additional paths for the current to flow from the grid to the soil. Fig. 12 locations of current injection points (corner and center) for a 40 m x 40 m grid with a 5 m x 5 m mesh size. The influence of the current injection point on the grid performance is investigated for different frequencies in low and high soil resistivity [23], [24], [22], [101].

Fig. 13 shows an assessment of the grid impedances at different soil resistivities for currents injected at the center and corner of the ground grid. At a low frequency, the current injection points exert no reaction, thus the impedance remains persistent for high and low soil resistivity. At a high frequency range, as the inductive effect becomes assertive, the impedance magnitude increases distinctly. The magnitude

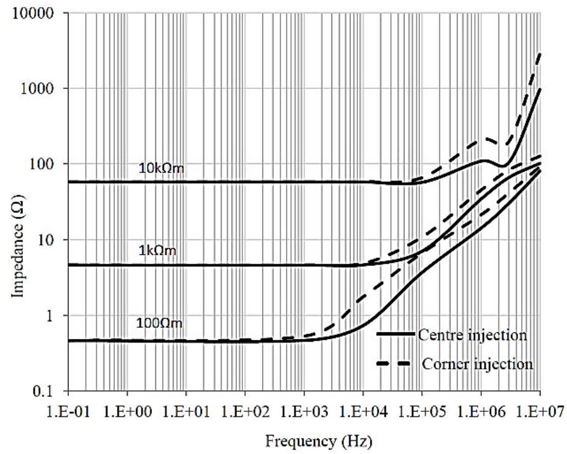

FIGURE 13. Ground grid impedance for the center and corner current injection points for different soil resistivities [83].

TABLE 9. Summary of effect of current injection point on grounding grid impedance.

Location of the injection point	Frequency	Soil resistivity	Effect of current injection point on grounding grid impedance
Corner	Low	Low	Almost constant
		High	Almost constant
	High	Low	Higher than the center injection point
		High	Higher than center injection point, higher magnitude compared to low resistivity
Center	Low	Low	Almost constant
		High	Almost constant
	High	Low	Lower than corner injection point
		High	Lower than corner injection point, higher magnitude compared to low resistivity

of impedance for current injected at the center of the grid is lower than for the corner injection point [94]. Table 9 shows the effects of current injection points on grid impedance.

B. EFFECT OF LIGHTNING CURRENT WAVEFORM

The front time of a lightning current waveform defines the frequency content of the current. Therefore, it is one of the critical components to consider in simulations. In simulations, different lightning currents including 1.2/50, 2.6/50 and 10/350 μs, are used to study the impact of lightning current waveforms on ground potential rise. The magnitude of the current is fixed at 10 kA. Thereafter, the currents are injected at the corner of a 20 m x 20 m grid with 5 m x 5 m mesh size. The grid is buried 0.5 m below the surface of the soil with 1000 Ω.m resistivity [23], [102].

Fig. 14 exhibits the potential rise at the injection points for varying impulse waveforms. The figure shows that a 1.2/50 μs front time generates almost double the potential relative to the 2.6/50 μs front time. A faster front time with a steeply-changing current can create a high potential rise

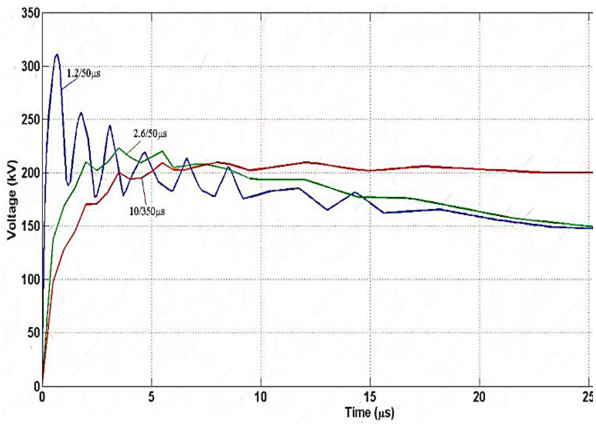

FIGURE 14. Potential rise for various front times [23].

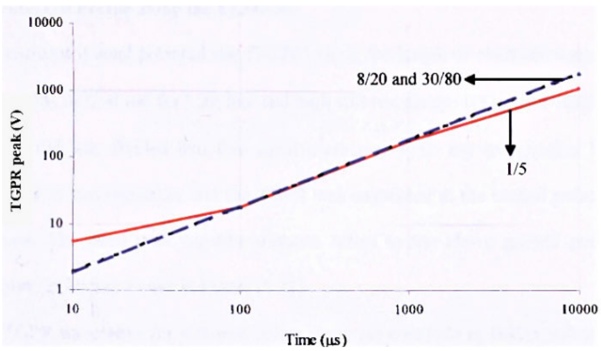

FIGURE 15. TGPR peak magnitude of the 5 m vertical electrode injected with different current impulses [103].

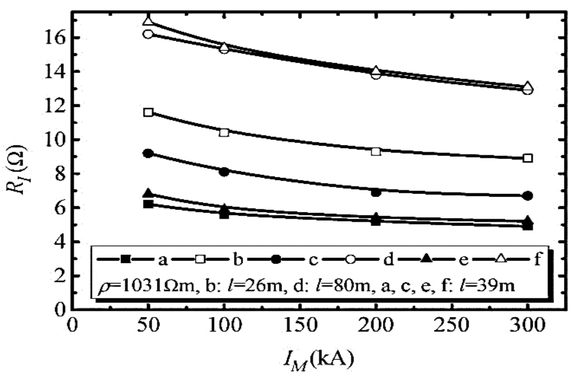

FIGURE 16. Effect of lightning current magnitude on the grounding resistance of different grounding devices [105].

because of high-frequency elements. This condition increases the impedance of the grounding system. The ripple is obvious and large for short front times possibly because of reflection of the wave when the impedance changes at the junction of the grid conductor or because of the numerical instability of the software. The reflection can be estimated by calculating the velocity of the electromagnetic wave.

The velocity of the electromagnetic wave can be estimated as 100 m/μs when the permittivity of soil, $\varepsilon_r = 9$. The first ripple occurs approximately at 1 μs as shown in Fig. 16; during reflection, the ripples form 50 m from the injection point. However, at 50 m from the injection point, the characteristic impedance does not change as the soil is homogenous.

TABLE 10. Summary of effects of lightning current waveforms on ground potential rise.

Current impulse	Soil resistivity	Effect of the current waveform on GPR
Fast (1/5μs)	Low	High
	High	Low
Slow (8/20μs) (30/80μs)	Low	Low
	High	High

Therefore, the ripple can be improved by refining the mesh size, especially for the shortest rise time to improve the numerical calculation. However, fine meshes require much computational time and memory [23].

Fig. 15 shows the connection between the transient ground potential rise (TGPR) peak magnitude and the current impulse for different soil resistivities. The TGPR values are compared across different impulse shapes namely; fast transient current impulse (1/5 μs), standard lightning current impulse (8/20 μs), and switching current impulse (30/80 μs). The graph shows that the 30/80 μs current impulse produces a TGPR peak magnitude that is equivalent to that produced by 8/20 μs current impulse. The TGPR peak magnitude is higher for 1/5 μs than for 8/20 μs and 30/80 μs under low soil resistivity, but it is generally low in a high soil resistivity medium. This result indicates that capacitive and inductive effects are obvious in a fast-transient impulse current. Moreover, the increment in TGPR peak magnitude is low as soil resistivity increases for a fast-transient impulse current (1/5 μs) relative to that for slow current impulses (8/20 μs and 30/80 μs). A summary of the effects of lightning current waveforms on the ground potential rise is presented in Table 10.

C. EFFECT OF LIGHTNING CURRENT MAGNITUDE

The effect of the peak value of lightning current on grounding resistance is shown in Fig. 16. The effect is analyzed using actual grounding devices enclosed with low resistivity materials (LRM) namely: type a: steel tower radial grounding device; type b: circular grounding device; type c: concrete tower radial grounding device; type d: horizontal grounding electrode; type e: horizontal grounding electrode with lightning injected in the middle point; type f: vertical grounding electrode.

The grounding resistance decreases as the lightning peak current increases until it reaches a saturation point. When the magnitude of lightning current exceeds a specific value, the grounding resistance still decreases gradually. A proper apprehension on this trend of saturation will help in designing lightning protection systems. For example, the potential on top of TL tower is linearly related to the current peak value when lightning hits a TL tower, [104], [105]. Grounding behaviors depend not only on grounding design and soil resistivity, yet also on the waveform and lightning current magnitude.

An extremely conductive channel will be formed around the electrode, when the strength of the electric field exceeds the dielectric strength of soil around a grounding electrode

TABLE 11. Summary of soil ionization models.

Soil Ionization model	The equation for ground resistance with soil ionization	Advantages	Disadvantages
CIGRE [110]	$$R_i = \frac{R}{\sqrt{1 + i(t)/I_g}}$$ where R is a grounding electrode resistance in [Ω], and $i(t)$ is the impulse current in [kA]. Ig is the limit current at which the soil ionization happens in [kA].	• simple • easily used in circuit approaches.	• only valid for a maximum of 30m long electrodes. • In computations, it does not consider the energy balance concept. • cannot show the hysteresis characteristic of grounding electrode resistance.
Bellaschi [111]	Considers the geometry of the ionized zone as the grounding electrode' new geometry because it considers the arc's resistance to zero. Consequently, the length and radius of the ionized region are used as the effective radius, a_i and effective length l_i of conductor. The following relation is considered for calculating the effective radius a_i,. $$a_i = \frac{a\, i(t)}{I_c}$$ where a, is the conductor radius in [m], i(t) is the magnitude of impulse current in [kA], and Ic is the critical current in [kA] where soil ionization occurs at the electrode surface. The relation of a_i to the current is used to calculate the conductor effective length, l_i as $$\frac{i\,(t)}{I_c} = \frac{a_i l_i}{al}$$	• can be used for a multi-electrode system. • simple and applicable to use in circuit approaches.	• does not consider the energy balance concept in the calculations
Nor [112]	$$R(t) = R_1(i)\left(\frac{R_2(i)}{R_1(i)} + e^{t/\tau_i}\right)$$ where τ_i is the time constant of ionization. Due to thermal effect and soil capacitive effect, resistance R_1 reflects the conduction of the soil in the pre-ionization branch. R_2 resistance represents the conduction performance in the post-ionization branch after the ionization is completely expanded.	• simple	• does not consider the deionization time. • cannot accurately predict the resistance characteristics for the decay time duration of the impulse current. • Difficult to obtain experimental data to obtain the resistances in the pre- and post-ionization branches. • cannot generate an accurate grounding electrode resistance and its voltage response, unless the experimental data is used to calibrate the model. • does not consider the energy balance concept because the model does not consider the deionization time.
Liew-Darveniza [113]	$$\rho = \rho_i + (\rho_0 - \rho_i).\left(1 - e^{-t/\tau_2}\right).(1 - J/J_c)^2$$ where ρ_i is the lowest soil resistivity value and τ_2 = 4.5 µs, the approximate recovery time. ρ_0 is the soil resistivity at the instance of current discharge. t, is the time measured from the ionization onset, J is the current density and J_c is the critical current density. $$R = \frac{\rho}{2\pi l}\ln\frac{a + l}{a}$$ where ρ is the soil resistivity in [Ω.m], l is the electrode length in [m], and a is the conductor radius in [m].	• considers the concept of energy balance. • exhibits the hysteresis characteristic of the grounding electrode resistance under impulse condition	• more complex. • In the equivalent circuit, the electrode inductance and soil capacitance are ignored. • cause large errors in electrode voltage response under fast and slow fronted currents when the inductive and capacitive characteristics are important.

which reduces ground impedance [74], [106], [107]. New empirical formulas estimating the effective area of grounding grids, the impulse coefficient, and impedance identify the parameters which are responsible for reducing surge performance of grounding grids as opposed to low-frequency performance. The concept of soil ionization models suggested by CIGRE, Bellaschi *et al.*, Nor *et al.*, and Liew and Darveniza have been explained well in [35], [49], [108]–[111]. The following Table 11 summarizes the equation, advantages, and disadvantages of the suggested models.

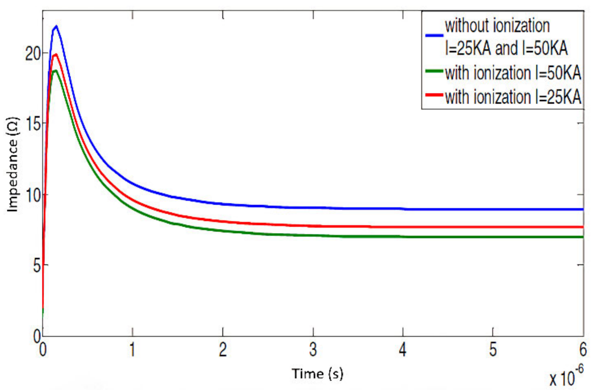

FIGURE 17. Effect of soil ionization on. transient impedance of grounding grid at. $\rho = 300\ \Omega$m [106].

This classification is not rigorous as indicated in [49], but is generally adopted in the literature for fundamental understanding.

A methodical simulation and analysis were conducted in [106] to compute the effect of soil ionization on the behavior of the grounding system. Fig. 17 shows the transient impedance (Z) of a 12 m x 12 m grounding grid, injected with 2/12 μs impulse at the center with and without soil ionization. As can be seen for 50 kA and 25 kA of lightning current in soil without ionization, the transient impedance of both cases has the same waveshape. However, comparing this to the cases which consider the influence of soil ionization, soil ionization decreases the voltage and thus decreases the grid impedance.

V. INFLUENCE OF SOIL IONIZATION ON TRANSIENT GROUNDING IMPEDANCE

Soil ionization is a nonlinear effect that is created by injecting high currents into concentrated grounding systems buried in high-resistivity soil. The effect of soil ionization is simulated by many methods such as the Finite Element (FEM) method, Finite Difference Time Domain (FDTD) method, and the Transmission-Line (TL) method.

VI. CONCLUSION

High frequency and transient conditions such as switching and lightning behaviors, are important to consider in grounding grid design. The analysis of grounding behavior in transient conditions helps to prevent high potential rise on the ground, which could be harmful to humans and damaging for power equipment. The development of modeling methods as mentioned in this article helps in a better understanding of grounding system theory and implementation in real equipment or practical scenarios. Furthermore, a basic understanding of computation and solution involved in modeling approaches enable the prediction of behavior and performance of grounding systems installed without worrying about damage and installation costs. The analysis of design parameters on grounding behavior provide useful direction for installing grounding electrodes and determining grounding systems' performances to obtain a safe and effective substation grounding system design. The investigation of grounding behaviors in different design parameters and also in transient conditions helps to prevent high potential rise on the ground, which could be harmful to humans and damaging for power equipment. the ground, which could be harmful to humans and damaging for power equipment. In addition, the characteristics of lightning also plays an important role while designing the grounding system. For example, a grid impedance which is in satisfactory range for a power frequency condition, might not be adequate for a safe working environment under lightning fault condition. The boundary of a substation should be located at a safe distance from the grounding grid as transient can be a disastrous for small grids and high soil resistivity medium due to high ground potential rise. Finally, under transient condition, soil ionization influences the value of the grounding impedance in transient conditions. It reduces the potential on the electrode which assumes significant changes to soil resistivity. This will significantly affect the design and performance of the grounding grid.

ACKNOWLEDGMENT

The authors would like to express their sincerest appreciation and thanks to Universiti Tenaga Nasional for the guidance given and for the financial support through UNITEN BOLD publication fund and UNITEN BOLD Postgraduate Scholarship Programme.

REFERENCES

[1] A. Taher, A. Said, T. Eliyan, and A. Hafez, "Optimum design of substation grounding grid based on grid balancing parameters using genetic algorithm," in *Proc. 20th Int. Middle East Power Syst. Conf. (MEPCON)*, Dec. 2018, pp. 352–360, doi: 10.1109/MEPCON.2018.8635109.
[2] *Grounding of Industrial and Commercial Power Systems*, IEEE Standard 142. 2007.
[3] V. Cooray, *Lightning Protection* (IET Power and Energy Series). London, U.K.: The Institution of Engineering and Technology, 2010.
[4] K. Y. A. Ametani, N. Nagaoka, Y. Baba, and T. Ohno, *Power System Transients: Theory & Application*, 2nd ed. Boca Raton, FL, USA: CRC Press, 2017.
[5] R. Anderson and A. J. Ericksson, "Lightning parameters for engineering application," Tech. Rep. CIGRE C4-407, no. 2004, 2013. [Online]. Available: https://e-cigre.org/publication/549-lightning-parameters-for-engineering–applications
[6] J. D. McDonald, *Electric Power Substations Engineering*. Boca Raton, FL, USA: CRC Press, 2009.
[7] N. Abdullah, A. M. A. Marican, M. Osman, and N. A. A. Rahman, "Case study on impact of seasonal variations of soil resistivities on substation grounding systems safety in tropical country," in *Proc. 7th Asia–Pacific Int. Conf. Lightning*, Nov. 2011, pp. 150–154, doi: 10.1109/APL.2011.6111092.
[8] T. R. Ayodele, A. S. O. Ogunjuyigbe, and O. E. Oyewole, "Comparative assessment of the effect of earthing grid configurations on the earthing system using IEEE and finite element methods," *Eng. Sci. Technol., Int. J.*, vol. 21, no. 5, pp. 970–983, Oct. 2018, doi: 10.1016/j.jestch.2018.07.003.
[9] A. Ganiyu and L. Akintola, "Power system faults: A hindrance to sustainability and reliability," *Int. J. Eng. Res.*, vol. 3, no. 11, pp. 700–703,2014, doi: 10.17950/ijer/v3s11/1116.
[10] *IEEE Guide for Safety in AC Substation Grounding*, Standard 80-2013, 2013.
[11] *Guide for Measuring Earth Resistivity, Ground Impedance, and Earth Surface Potentials of a Grounding System*, IEEE Standard 81-2012, 2012.
[12] *Code of Practice for Protective Earthing of Electrical Installations*, document BS7430:2011, 2011.
[13] *Power Installations Exceeding 1 kV A.C. Common Rules*, document IS EN 61936:1-2010, 2010.
[14] *Substation Lightning Protection, Substation Lightning Protection Asset Class Strategy Intellectual*, document 1-11-ACS-11,2018.
[15] J. Montaña, "Recommendations for grounding systems in lightning protection systems," *Ingeniería e Investigación*, vol. 31, no. 2, pp. 5–10, 2011, doi: 10.15446/ing.investig.

[16] S. Dahal, R. Martin, and S. Paudyal, "Impact of lightning strikes on substation grounding systems," in *Proc. Australas. Universities Power Eng. Conf. (AUPEC)*, Nov. 2017, pp. 1–5, doi: 10.1109/AUPEC.2017.8282407.

[17] H. N. Amadi, "Design of grounding system for AC substations with critical consideration of the mesh, touch and step potentials," *Eur. J. Eng. Technol.*, vol. 5, no. 4, pp. 44–57, 2017.

[18] S. D. Buba, W. F. Wan Ahmad, M. Z. A. Ab Kadir, C. Gomes, J. Jasni, and M. Osman, "Reduction of earth grid resistance by addition of earth rods to various grid configurations," *ARPN J. Eng. Appl. Sci.*, vol. 11, no. 7, pp. 4533–4538, 2016.

[19] S. D. Buba, W. F. Wan Ahmad, M. Z. A. Ab Kadir, C. Gomes, J. Jasni, and M. Osman, "Effect of Earth grid conductor spacing on the safety criteria of substation earthing," in *Proc. IEEE Int. Conf. Power Energy (PECon)*, Dec. 2014, pp. 134–139, doi: 10.1109/PECON.2014.7062428.

[20] D. Buba, W. F. Wan Ahmad, M. Z. A. Ab Kadir, C. Gomes, J. Jasni, and M. Osman, "Impact of energization current on the safe design of distribution substation Earth grid," in *Proc. IEEE Int. Conf. Power Energy (PECon)*, Dec. 2014, pp. 201–205, doi: 10.1109/PECON.2014.7062441.

[21] H. Chen, Y. Zhang, Y. Du, and Q. S. Cheng, "Lightning transient analysis of telecommunication system with a tubular tower," *IEEE Access*, vol. 6, pp. 60088–60099, 2018, doi: 10.1109/ACCESS.2018.2875723.

[22] F. Bin Hanaffi and W. H. Siew, "Boundary analysis on transient grounding modelling using FEM," in *Proc. 8th Asia–Pacific Int. Conf. Lightning*, 2017, pp. 1–4.

[23] F. Hanaffi, W. H. Siew, I. Timoshkin, H. Lu, Y. Wang, L. Lan, and X. Wen, "Evaluation of grounding grid's effective area," in *Proc. Int. Conf. Lightning Protection (ICLP)*, Oct. 2014, pp. 402–406, doi: 10.1109/ICLP.2014.6973157.

[24] W. H. Siew and F. Bin Hanaffi, "Transient grounding modelling using FEM: Infinite boundary condition," in *Proc. CIGRE Int. Colloq. Lightning Power Syst.*, no. 1, pp. 1–5, Mar. 2014.

[25] G. Singh, "Design of grounding system for an electrical substation: An overview," *Int. J. Sci. Eng. Res.*, vol. 5, no. 11, pp. 246–248, 2014.

[26] N. Çetinkaya and F. Umer, "Effect of neutral grounding protection methods for compensated wind/PV grid-connected hybrid power systems," *Int. J. Photoenergy*, vol. 2017, Nov. 2017, Art. no. 4860432, doi: 10.1155/2017/4860432.

[27] S. Polstyanko, "A comparison of IEC 479-1 and IEEE Std 80 on grounding safety criteria," *Adv. Psychol.*, vol. 2000, pp. 1–4, Dec. 2010, doi: 10.1109/20.952557.

[28] M. Mondal, R. K. Jarial, S. Ram, and G. Singh, "Design and analysis of substation grounding grid with and without considering seasonal factors using EDSA software," *Int. J. Innov. Eng. Technol.*, pp. 64–77, 2013, doi: 10.1109/sces.2013.6547527.

[29] L. Grcev and V. Arnautovski-Toseva, "Grounding systems modeling for high frequencies and transients: Some fundamental considerations," in *Proc. IEEE Bologna Power Tech Conf.*, Jun. 2003, pp. 1020–1026, doi: 10.1109/PTC.2003.1304516.

[30] H. Widyaputera, "Modelling and touch voltage simulation of various earth grid configuration against lightning," *Int. J. Power Syst.*, pp. 1–7, 2019.

[31] J. Bandel, A. Hejduk, A. Dzierżyński, P. Korycki, and H. Sibilski, "Switching and lightning overvoltages and the required withstand voltage betweeen the open contacts OF 245 KV circuit breakers," *Proc. Electrotech. Inst.*, vol. 63, pp. 43–60, Dec. 2016, doi: 10.5604/01.3001.0009.4410.

[32] D. Lian, Z. Bo, H. Jinliang, X. Leishi, and L. Qian, "Experimental study on transient characteristics of grounding grid for substation," in *Proc. 33rd Int. Conf. Lightning Protection (ICLP)*, Sep. 2016, pp. 1–6, doi: 10.1109/ICLP.2016.7791392.

[33] G. Delvare, "A review of methods for grounding grid analysis," in *Proc. 17th Int. Conf. Softw., Telecommun. Comput. Netw.*, 2014, pp. 42–49.

[34] P. Jacqmaer and J. L. Driesen, "Modelling of grounding systems with the method of moments," *IEEE Benelux Young Res. Symp. Electr. Power Eng.*, no. 32, pp. 1–10, 2006.

[35] H. Chen and Y. Du, "Lightning grounding grid model considering both the frequency-dependent behavior and ionization phenomenon," *IEEE Trans. Electromagn. Compat.*, vol. 61, no. 1, pp. 157–165, Feb. 2019, doi: 10.1109/TEMC.2017.2789210.

[36] G. Celli, E. Ghiani, and F. Pilo, "Behaviour of grounding systems: A quasi-static EMTP model and its validation," *Electr. Power Syst. Res.*, vol. 85, pp. 24–29, Apr. 2012, doi: 10.1016/j.epsr.2011.07.004.

[37] P. Yutthagowith, A. Ametani, N. Nagaoka, and Y. Baba, "Application of the partial element equivalent circuit method to analysis of transient potential rises in grounding systems," *IEEE Trans. Electromagn. Compat.*, vol. 53, no. 3, pp. 726–736, Aug. 2011, doi: 10.1109/TEMC.2010.2077676.

[38] M. Mokhtari, Z. Abdul-Malek, and Z. Salam, "An improved circuit-based model of a grounding electrode by considering the current rate of rise and soil ionization factors," *IEEE Trans. Power Del.*, vol. 30, no. 1, pp. 211–219, Feb. 2015, doi: 10.1109/TPWRD.2014.2347283.

[39] P. Yutthagowith, "A modified pi-shaped circuit-based model of grounding electrodes," in *Proc. 33rd Int. Conf. Lightning Protection (ICLP)*, Sep. 2016, pp. 1–4, doi: 10.1109/ICLP.2016.7791379.

[40] A. P. Meliopoulos and M. G. Moharam, "Transient analysis of grounding systems," *IEEE Trans. Power App. Syst.*, vol. 3, no. 3, pp. 1220–1222, May 2013, doi: 10.1016/j.cor.2015.02.003.

[41] B. Zhang, J. Wu, J. He, and R. Zeng, "Analysis of transient performance of grounding system considering soil ionization by time domain method," *IEEE Trans. Magn.*, vol. 49, no. 5, pp. 1837–1840, May 2013, doi: 10.1109/TMAG.2013.2243824.

[42] P. Papalexopoulos, "Frequency dependent characteristics of grounding systems," *IEEE Trans. Power Del.*, vol. PWRD-2, no. 3, pp. 531–537, Oct. 1985, doi: 10.1177/1553350613503735.

[43] M. Ramamoorty, M. M. B. Narayanan, S. Parameswaran, and D. Mukhedkar, "Transient performance of grounding grids," *IEEE Power Eng. Rev.*, vol. 9, no. 10, p. 48, Oct. 1989.

[44] A. Geri, "Behaviour of grounding systems excited by high impulse currents: The model and its validation," *IEEE Trans. Power Deliv.*, vol. 14, no. 3, pp. 1008–1017, Jul. 1999, doi: 10.1109/61.772347.

[45] R. Rudenberg, *Electrical Shock Waves in Power Systems*. Cambridge, MA, USA: Harvard Univ. Press, 1986.

[46] O. E. Gouda, *Design Parameters of Electrical Network Grounding Systems*. 2018, pp. 291–292.

[47] S. Mousa, N. Harid, H. Griffiths, and A. Haddad, "Experimental investigation on high-frequency and transient performance of a vertical earth electrode," in *Proc. 46th Int. Univ. Power Eng. Conf. (UPEC)*, vol. 1, Sep. 2011, pp. 4–7.

[48] M. Lefouili, Z. Belli, K. Kerroum, and K. El Khamlichi Drissi, "Computational model of grounding systems," in *Proc. Int. Conf. Lightning Protection (ICLP)*, Sep. 2012, pp. 1–5, doi: 10.1109/ICLP.2012.6344213.

[49] M. Mokhtari, Z. Abdul-Malek, and G. B. Gharehpetian, "A critical review on soil ionisation modelling for grounding electrodes," *Arch. Electr. Eng.*, vol. 65, no. 3, pp. 449–461, Sep. 2016, doi: 10.1515/aee-2016-0033.

[50] M. Mokhatri and Z. Abdul-Malek, "The effect of grounding electrode parameters on soil ionization and transient grounding resistance using electromagnetic field approach," *Appl. Mech. Mater.*, vol. 554, pp. 628–632, Jun. 2014.

[51] R. Verma, "Impulse impedance of buried ground wire," *IEEE Trans. Power App. Syst.*, vol. PAS-99, no. 5, pp. 2003–2007, Sep. 2003.

[52] G. Ala and M. L. Di Silvestre, "A simulation model for electromagnetic transients in lightning protection systems," *IEEE Trans. Electromagn. Compat.*, vol. 44, no. 4, pp. 539–554, Nov. 2002, doi: 10.1109/TEMC.2002.804773.

[53] P. Wang, L. Li, and V. A. Rakov, "Calculation of current distribution in the lightning protective system of a residential house," *IEEE Trans. Magn.*, vol. 50, no. 2, Feb. 2014, Art. no. 7005404, doi: 10.1109/TMAG.2013.2283257.

[54] D. Sekki, B. Nekhoul, K. Kerroum, K. E. K. Drissi, and D. Poljak, "Transient behaviour of grounding system in a two-layer soil using the transmission line theory," *Automatika*, vol. 55, no. 3, pp. 306–316, 2014, doi: 10.7305/automatika.2014.12.497.

[55] A. Bhasin and S. C. Sharma, "Time-domain modeling of grounding systems' impulse response incorporating nonlinear and frequency-dependent aspects," *IEEE J. Quantum Electron.*, vol. 47, no. 5, pp. 751–752, May 2011, doi: 10.1109/JQE.2010.2101053.

[56] S. Chiheb, O. Kherif, M. Teguar, and A. Mekhaldi, "Transient behavior of vertical grounding electrode under impulse current," in *Proc. 5th Int. Conf. Electr. Eng.-Boumerdes (ICEE-B)*, Oct. 2017, pp. 1–5, doi: 10.1109/ICEE-B.2017.8192075.

[57] C. Mazzetti and G. Veca, "Impulse behavior of ground electrodes," *IEEE Trans. Power App. Syst.*, vol. PAS-102, no. 9, pp. 3148–3156, Sep. 1983, doi: 10.1109/tpas.1983.318122.

[58] M. I. Lorentzou, N. D. Hatziargyriou, and B. C. Papadias, "Time domain analysis of grounding electrodes impulse response," *IEEE Trans. Power Del.*, vol. 18, no. 2, pp. 517–524, Apr. 2003, doi: 10.1109/tpwrd.2003.809686.

[59] M. Mokhtari, "Circuit based transient model of grounding electrode with consideration of soil ionization and current-rate-of-rise factors," Ph.D. dissertation, Dept. Elect. Eng., Univ. Teknologi Malaysia, Johor Bahru, Malaysia, 2016.

[60] Y. Liu, N. Theethayi, and R. Thottappillil, "An engineering model for transient analysis of grounding system under lightning strikes: Nonuniform transmission-line approach," *IEEE Trans. Power Del.*, vol. 20, no. 2, pp. 722–730, Apr. 2005, doi: 10.1109/tpwrd.2004.843437.

[61] D. Poljak and V. Doric, "Wire antenna model for transient analysis of simple grounding systems, Part II: The horizontal grounding electrode," *Prog. Electromagn. Res.*, vol. 64, pp. 167–189, 2006, doi: 10.2528/PIER06062102.

[62] R. Araneo, M. Maccioni, S. Lauria, A. Geri, F. Gatta, and S. Celozzi, "Hybrid and pi-circuit approaches for grounding system lightning response," in *Proc. IEEE Eindhoven PowerTech*, Jun. 2015, pp. 1–6, doi: 10.1109/PTC.2015.7232419.

[63] M. Chouki, B. Nekhoul, and K. Kerroum, "Transient electromagnetic field radiated by buried electrode," in *Proc. 10th Int. Symp. Electromagn. Compat.*, Sep. 2011, pp. 615–618.

[64] A. Manunza, "Grounding grids in electro-magnetic transient simulations with frequency-dependent equivalent circuit," *Int. J. Electr. Power Energy Syst.*, vol. 116, Mar. 2020, Art. no. 105546, doi: 10.1016/j.ijepes.2019.105546.

[65] L. Grcev, "Time- and frequency-dependent lightning surge characteristics of grounding electrodes," *IEEE Trans. Power Del.*, vol. 24, no. 4, pp. 2186–2196, Oct. 2009, doi: 10.1109/TPWRD.2009.2027511.

[66] N. Mohamad Nor, S. Abdullah, R. Rajab, and K. Ramar, "Field tests: Performances of practical earthing systems under lightning impulses," *Int. J. Electr. Power Energy Syst.*, vol. 45, no. 1, pp. 223–228, Feb. 2013, doi: 10.1016/j.ijepes.2012.08.077.

[67] "Analysis of wire antennas in the presence of a conductive half space: Part III: The buried antenna," to be published.

[68] K. Nagarjuna and K. Chandrasekaran, "Analysis of horizontal grounding electrode in transmission line approach," in *Proc. Int. Conf. Commun. Electron. Syst. (ICCES)*, Jul. 2019, pp. 267–272, doi: 10.1109/ICCES45898.2019.9002144.

[69] K. Tanabe and A. Asakawa, "Computer analysis of transient performance of grounding grid element based on the finite-difference time-domain method," in *Proc. IEEE Int. Symp. Electromagn. Compat.*, vol. 1, May 2003, pp. 209–212, doi: 10.1109/icsmc2.2003.1428231.

[70] L. Zhiwei and Z. Zhao, "The grounding impedance calculation of large steel grounding grid," *Energy Procedia*, vol. 17, pp. 157–163, 2012, doi: 10.1016/j.egypro.2012.02.077.

[71] B. Zhang, J. He, J.-B. Lee, X. Cui, Z. Zhao, J. Zou, and S.-H. Chang, "Numerical analysis of transient performance of grounding systems considering soil ionization by coupling moment method with circuit theory," *IEEE Trans. Magn.*, vol. 41, no. 5, pp. 1440–1443, May 2005, doi: 10.1109/TMAG.2005.844547.

[72] R. Araneo and S. Celozzi, "Transient behavior of wind towers grounding systems under lightning strikes," *Int. J. Energy Environ. Eng.*, vol. 7, no. 2, pp. 235–247, Jun. 2016, doi: 10.1007/s40095-015-0196-7.

[73] J. Meppelink, "Calculation models for grounding systems based on hybrid methods," *SINT Ingegneria Srl*, no. 1, pp. 1–9, Dec. 2015, doi: 10.13140/RG.2.1.3571.8481.

[74] D. S. Gazzana, A. S. Bretas, D. W. P. Thomas, and C. Christopoulos, "A hybrid method to represent the soil ionization phenomenon in impulsive grounding systems," in *Proc. IEEE Conf. Electromagn. Field Comput. (CEFC)*, Nov. 2016, p. 1, doi: 10.1109/CEFC.2016.7815924.

[75] S. Visacro and A. Soares, "HEM: A model for simulation of lightning-related engineering problems," *IEEE Trans. Power Del.*, vol. 20, no. 2, pp. 1206–1208, Apr. 2005, doi: 10.1109/TPWRD.2004.839743.

[76] F. Dawalibi, "Electromagnetic fields generated by overhead and buried short conductors part 2-ground networks," *IEEE Power Eng. Rev.*, vol. PER-6, no. 10, pp. 34–35, Oct. 1986, doi: 10.1109/MPER.1986.5527603.

[77] A. H. D. Warne, "Earthing," in *Advances in High Voltage Engineering*. London, U.K.: Institution of Engineering and Technology, 2007, pp. 349–350.

[78] H. A. Hasan and S. M. Hameed, "Characteristics of earth electrodes under high frequency conditions: Numerical modelling," in *Proc. IOP Conf., Mater. Sci. Eng.*, 2020, vol. 671, no. 1, Art. no. 012043, doi: 10.1088/1757-899X/671/1/012043.

[79] *Guidelines for the Design, Installation, Testing and Maintenance of Main Earthing Systems in Substations*, document EA TS 41-24:2017, 2017.

[80] H. F. B. Van der Linde Zedan, "Impulse Response of Earth Electrode Systems," in *Proc. 37th Int. Universities Power Eng. Conf. (UPEC)*, Stafford, U.K., 2002, pp. 827–831.

[81] M. U. Aslam, M. U. Cheema, M. B. Cheema, and M. Samran, "Design analysis and optimization of ground grid mesh of extra high voltage substation using an intelligent software," in *Proc. 1st Int. Conf. Inf. Technol., Comput., Electr. Eng.*, Nov. 2014, pp. 339–345, doi: 10.1109/ICITACEE.2014.7065768.

[82] A. H. F. van der Linde, B. Zedan, and H. Griffiths, "The impulse response of earth grid," in *Proc. 13th Int. Symp. High Voltage Eng.*, 2003, pp. 119–123.

[83] A. El Mghairbi, M. Ahmeda, N. Harid, H. Griffiths, and A. Haddad, "Technique to increase the effective length of practical Earth electrodes: Simulation and field test results," *Electr. Power Syst. Res.*, vol. 94, pp. 99–105, Jan. 2013, doi: 10.1016/j.epsr.2012.04.015.

[84] A. Dimopoulos, H. Griffiths, A. Haddad, A. Ainsley, F. Ainslie, and D. Frame, "Parametric analysis of safety limit-curves in earthing systems and comparison of international standard recommendations," in *Proc. 41st Int. Universities Power Eng. Conf.*, Sep. 2006, pp. 272–276, doi: 10.1109/upec.2006.367758.

[85] H. Griffiths, A. Haddad, and N. Harid, "Characterisation of earthing systems under high frequency and transient conditions," in *Proc. 39th Int. Univ. Power Eng. Conf.*, vol. 1, Sep. 2004, pp. 188–192.

[86] Z. B. Feng, C. S. Wang, J. Xia, and L. Wang, "A new method of grounding grid design," im *Proc. MATEC Web Conf.*, vol. 59, 2016, pp. 1–5, doi: 10.1051/matecconf/20165902003.

[87] M. Abdallah, "The effect of grid mesh density on substation earth impedance," in *Proc. 36th Univ. Power Eng. Conf. (UPEC)*, Swansea, U.K., 2005, pp. 443–447.

[88] B. Zedan, "Characterisation of Substation Earth Grid under High Frequency and Transient Conditions," Ph.D. dissertation, School Eng., Cardiff Univ., Cardiff, U.K., 2005.

[89] A. Puttarach, N. Chakpitak, T. Kasirawat, and C. Pongsriwat, "Substation grounding grid analysis with the variation of soil layer depth method," in *Proc. IEEE Lausanne Power Tech*, Jul. 2007, pp. 1881–1886, doi: 10.1109/PCT.2007.4538604.

[90] S. C. Malanda, I. E. Davidson, E. Singh, and E. Buraimoh, "Analysis of soil resistivity and its impact on grounding systems design," in *Proc. IEEE PES/IAS PowerAfrica*, Jun. 2018, pp. 324–329, doi: 10.1109/PowerAfrica.2018.8520960.

[91] Y. Meng, W. Chen, C. Liu, X. Luo, X. Huang, and H. Tan, "Influence of grounding design around down lead on lightning impulse behavior of substation grounding grid," in *Proc. 11th Asia–Pacific Int. Conf. Lightning (APL)*, Jun. 2019, pp. 3–6, doi: 10.1109/APL.2019.8816049.

[92] H. E. Messaoudi, O. Kherif, S. Chiheb, M. Teguar, and A. Mekhaldi, "Modelling of vertical ground electrode under lightning transient," in *Proc. 19th Int. Symp. Electromagn. Fields Mechatronics, Electr. Electron. Eng. (ISEF)*, Aug. 2019, pp. 6–7, doi: 10.1109/ISEF45929.2019.9097000.

[93] L. Zhou, J. He, H. Xu, P. Wang, Y. Chen, and S. Chen, "Simulation of impact of vertical grounding electrode on impulse grounding resistance of substation grounding network," in *Proc. 2nd IEEE Int. Conf. Integr. Circuits Microsyst. (ICICM)*, Nov. 2017, pp. 18–22, doi: 10.1109/ICAM.2017.8242130.

[94] A. Griffiths, B. Zedan, and H. Haddad, "Frequency response of earthing systems," in *Proc. 28th Int. Univ. Power Eng. Conf. (UPEC)*, 2003, pp. 717–720.

[95] M. Nayel, J. Zhao, J. He, Z. Cai, and Q. Wang, "Study of step and touch voltages in Resistive/Capacitive ground due to lightning stroke," in *Proc. 4th Asia–Pacific Conf. Environ. Electromagn.*, Aug. 2006, pp. 56–60, doi: 10.1109/CEEM.2006.257906.

[96] A. H. and A. A. H. H. Zhao Griffiths, "Safety-limit curves for earthing system designs: appraisal of standard recommendations," *IEE Proc.-Gener., Transmiss. Distrib.*, vol. 152, no. 6, pp. 871–879, 2005, doi: 10.1049/ip-gtd:20050007.

[97] N. Rameli, M. Z. A. Ab Kadir, M. Izadi, C. Gomes, and N. Azis, "Effect of soil resistivity on the lightning current along tall towers," in *Proc. Int. Conf. Lightning Protection (ICLP)*, Oct. 2014, pp. 451–455, doi: 10.1109/ICLP.2014.6973166.

[98] S. G. Shah and N. R. Bhasme, "Design of Earthing system for HV/EHV AC substation," *Int. J. Adv. Eng. Technol.*, vol. 6, no. 6, pp. 2597–2605, 2014.

[99] M. Lehtonen, M. Pichler, and R. Schurhuber, "Ground potential rise and lightning overvoltages in control systems of large power-plants under high soil resistivity," in *Proc. 20th Int. Sci. Conf. Electr. Power Eng. (EPE)*, May 2019, pp. 44–47, doi: 10.1109/EPE.2019.8777955.

[100] F. Hanaffi, W. H. Siew, and I. Timoshkin, "Step voltages in a ground-grid arising from lightning current," in *Proc. Asia–Pacific Int. Conf. Lightning (APL)*, Nagoya, Japan, Mar. 2015, pp. 264–267.
[101] L. Mghairbi, "Assessment of earthing systems and enhancement of their performance," Ph.D. dissertation, School Elect. Eng., Cardiff Univ., Cardiff, U.K., 2012.
[102] X. Tong, X. Dong, and B. Tan, "High current field test of impulse transient characteristics of substation grounding grid," *J. Eng.*, vol. 2019, no. 16, pp. 2018–2021, Mar. 2019, doi: 10.1049/joe.2018.8826.
[103] J. van der Linde, F. Zedan, B. Griffiths, H. Haddad, A. Walker, K. Frame, D. MacDonald, N. Horne, C. Porter, "Impulse response of earth electrode systems," in *Proc. 37th Int. Univ. Power Eng. Conf. (UPEC)*, 2002, pp. 965–969.
[104] L. M. Wai, M. S. A. Rahman, A. M. Ariffin, N. H. N. Ali, M. Osman, and M. Z. A. A. Kadir, "Evaluation of transient response of different earthing configurations due to lightning impulses," *Int. J. Recent Technol. Eng.*, vol. 8, no. 4, pp. 6342–6346, 2019, doi: 10.35940/ijrte.d5118.118419.
[105] Y. Tu, J. He, and R. Zeng, "Lightning impulse performances of grounding devices covered with low-resistivity materials," *IEEE Trans. Power Del.*, vol. 21, no. 3, pp. 1706–1713, Jul. 2006, doi: 10.1109/TPWRD.2006.874110.
[106] I. Djamel, F. H. Slaoui, and S. Georges, "Analysis of the transient behavior of grounding systems with consideration of soil ionization," in *Proc. 15th Int. Conf. Eur. Energy Market (EEM)*, Jun. 2018, pp. 1–5.
[107] L. K. Sing, N. Yahaya, S. R. Othman, S. N. Fariza, and N. M. Noor, "Substation grounding grid analysis with the variation of soil layer depth method," *J. Corros. Sci. Eng.*, vol. 6, no. 1, pp. 1–7, 2016, doi: 10.1109/PCT.2007.4538604.
[108] M. M. Z. A.-M. and Z. Salam, "The effect of soil ionization on transient grounding electrode resistance in non-homogeneous soil conditions," *Int. Trans. Elect. Energy Syst.*, vol. 26, no. 7, pp. 1462–1475, Jul. 2016, doi: 10.1002/etep.
[109] M. Mokhtari and G. B. Gharehpetian, "Integration of energy balance of soil ionization in CIGRE grounding electrode resistance model," *IEEE Trans. Electromagn. Compat.*, vol. 60, no. 2, pp. 402–413, Apr. 2018, doi: 10.1109/TEMC.2017.2731807.
[110] S. Sekioka, "Frequency and current-dependent grounding resistance model for lightning surge analysis," *IEEE Trans. Electromagn. Compat.*, vol. 61, no. 2, pp. 419–425, Apr. 2019, doi: 10.1109/TEMC.2018.2829923.
[111] B. Thangabalan and S. Das, "The effect of lightning on insulator flashover characteristics," in *Proc. 2nd Int. Conf. Power, Energy Environ., Towards Smart Technol. (ICEPE)*, no. 2, Jun. 2018, pp. 1–6, doi: 10.1109/EPETSG.2018.8658699.
[112] CIGRE Working Group 33-01 (Lightning) of Study Committee 33: Overvoltage and Insulation Coordination, "Guide to procedures for estimating the lightning performance of transmission lines," CIGRE, Paris, France, CIGRE Rep. 63, Oct. 1991, vol. 1, p. 64.
[113] P. L. Bellaschi and R. E. Armington, "Impulse and 60-cycle characteristics of driven grounds—II," *Trans. Amer. Inst. Electr. Eng.*, vol. 61, no. 6, pp. 349–363, 1942.
[114] N. Mohamad Nor, S. Abdullah, R. Rajab, and Z. Othman, "Comparison between utility sub-station and imitative earthing systems when subjected under lightning response," *Int. J. Electr. Power Energy Syst.*, vol. 43, no. 1, pp. 156–161, Dec. 2012, doi: 10.1016/j.ijepes.2012.04.042.
[115] J. P. Wang, A. C. Liew, and M. Darveniza, "Extension of dynamic model of impulse behavior of concentrated grounds at high currents," *IEEE Trans. Power Del.*, vol. 20, no. 3, pp. 2160–2165, Jul. 2005, doi: 10.1109/TPWRD.2004.839645.

NAVINESSHANI PERMAL received the Bachelor of Electrical and Electronics Engineering degree and the master's degree in electrical engineering from Universiti Tenaga Nasional, Malaysia, in 2014 and 2018, respectively, where she is currently pursuing the Ph.D. degree in electrical engineering. She is currently a Research Assistant with Universiti Tenaga Nasional. She has been actively involved in engineering related projects, such as Partial Discharge Detection Technique and Location Accuracy, Development of Bird Deterrent system through Phased Array Beamforming method, and analyzing the Impact of Lightning on Substation Grounding Performance in Non-Homogenous Soil. Her research interests include power system grounding and transient analysis.

MISZAINA OSMAN (Senior Member, IEEE) received the Bachelor of Electrical Engineering degree and the Ph.D. degree in electrical engineering from the University of Southampton, U.K., in 1999 and 2004, respectively. She has served as the Head of the Department of Electrical Power Engineering, from 2009 to 2011, and the Deputy Dean (Academic and Quality Assurance) and the Deputy Dean (Student Affairs and External Relations) with the College of Engineering, Universiti Tenaga Nasional (UNITEN), from 2011 to 2018. She is currently an Associate Professor with the Institute of Power Engineering, UNITEN. Her research interests include power system grounding, lightning protection, and high-voltage engineering. She is currently a member in the National Mirror Committee of IEC TC81 (Lightning Protection) and a country's Representative to the IEC TC 81 Meeting, for which Malaysia is a Permanent Member. She is also a member in the CIGRE Working Group C4.50 on Evaluation of Transient Performance of Grounding System in Substation. She is also a Professional Engineer (P. Eng.) and a Chartered Engineer (C.Eng.), as well as a member of the Institute of Engineering and Technology (IET), U.K., and The Institution of Engineers Malaysia (IEM).

MOHD ZAINAL ABIDIN AB. KADIR (Senior Member, IEEE) received the Bachelor of Engineering degree in electrical and electronic engineering from Universiti Putra Malaysia and the Ph.D. degree in high voltage engineering from the University of Manchester, U.K. He is currently a Strategic Hire Professor with the Institute of Power Engineering (IPE), Universiti Tenaga Nasional (UNITEN), and a Professor with the Faculty of Engineering, Universiti Putra Malaysia. He is also the Founding Director of the Center for Electromagnetic and Lightning Protection Research (CELP), Universiti Putra Malaysia. He is also an IEEE Power and Energy Society (PES) Distinguished Lecturer in the field of lightning and high voltage engineering. To date, he has authored or coauthored over 350 journals and conference papers. His research interests include high-voltage engineering, lightning protection, electromagnetic compatibility, and power system transients. He is a Professional Engineer (P.Eng.), a Chartered Engineer (C.Eng.), and a Professional Technologist (P.Tech.).

AZRUL MOHD ARIFFIN (Member, IEEE) received the Bachelor of Engineering degree (Hons.) in electrical engineering and the Ph.D. degree from the University of Southampton, U.K., in 2004 and 2008, respectively. His thesis investigated the electroluminescence phenomenon in insulating polymers subjected to the high-electric field. He is currently an Associate Professor and the Director of the Programme Management Office, Universiti Tenaga Nasional (UNITEN), Malaysia. He is also a Professional Engineer (P.Eng.) registered with the Board of Engineers (BEM), Malaysia.